

**Visualization of gold and uranium
ore-formation in the Witwatersrand
ore deposit from the micro- to nanoscale**
ZEISS Atlas 5

Visualization of gold and uranium ore-formation in the Witwatersrand ore deposit from the micro- to nanoscale

ZEISS Atlas 5

Authors: Dr. Sebastian Fuchs
Marine Mineral Resources
 GEOMAR Helmholtz Centre for Ocean Research Kiel
 Wischhofstr. 1-3, Geb. 8A-112; 24148 Kiel, Germany

Dr. Dirk Schumann and Andrew Murray
Fibics Incorporated, 1431 Merivale Road, Ottawa,
ON K2E 0B9, Canada

Date: July 2018

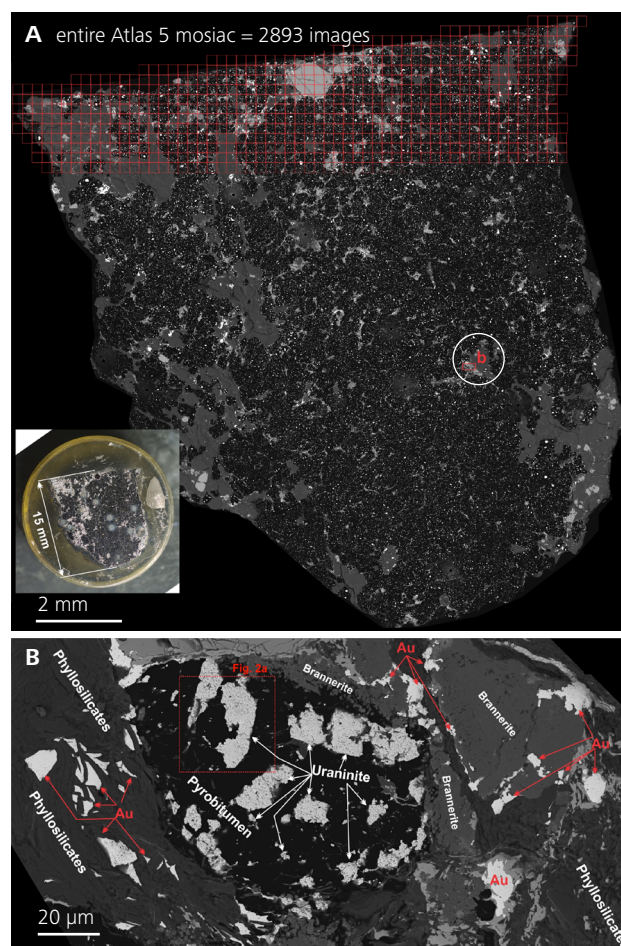
The Witwatersrand basin in South Africa represents the largest known gold resource on Earth. Despite decades of intensive research, the genesis of the gold-uranium ore is a matter of considerable debate. An analytical approach using the novel Atlas 5 workflow visualizes the process of gold and uranium ore-formation, from micro-to-nanoscale in both 2D and 3D, and uncovers the key-role of hydrocarbons in the metallogenesis.

Introduction

Researcher Sebastian Fuchs from the GEOMAR - Helmholtz Centre of Ocean Research Kiel (Germany) and his colleagues recently published a study in the scientific journal "Precambrian Research" providing an explanation for the formation of gold and uranium ore associated with fossil hydrocarbons in the Witwatersrand basin.

This study made use of a novel workflow for the characterization of geological samples including large area scanning-electron microscope (SEM) imaging, focused-ion beam SEM (FIB-SEM) nanotomography, and scanning-transmission electron microscope (S)TEM analyses, which revealed some striking evidence for the interaction of two immiscible fluids, namely hydrothermal and hydrocarbon liquids (oils), and the formation of micro-emulsions that led to the deposition of native gold and uraninite. The researchers made the case for an extensive mobilization of gold in hot aqueous fluids and the mobilization of uranium in hydrocarbon fluids and propose a unifying mineralization model that explains the association of the two metals in the carbon seams.

Figure 1 Backscattered electron (BSE) SEM images of a Carbon Leader Reef sample. (A) Atlas 5 large-area SEM image mosaic of the entire sample. (B) Higher-resolution SEM-BSE image mosaic of area "b" in image (A). The image shows pyrobitumen nodules that contain irregularly shaped uraninite grains.



The formation of gold and uranium ore in the Witwatersrand deposits

The Mesoarchean Witwatersrand basin, in the central part of the Kaapvaal Craton in South Africa, is a 7.5 km thick sequence of metasedimentary rocks including quartzites, shales, and conglomerates. The highest concentration of gold and uraninite occur in conglomerate units, also called “reefs” (minable units). The close spatial association of seams of organic matter with these reefs indicates a major role in the ore-forming process. The formation of gold and uranium ore in the Witwatersrand is matter of an ongoing debate, with opinion being generally divided over whether they are paleoplacers that are hydrothermally remobilized or entirely hydrothermal in origin. The origin of the hydrocarbon seams in the Witwatersrand is under considerable debate. Some studies interpreted the carbon seams to be remnants of algal (microbial) mats that formed during or shortly after sedimentation (Hallbauer, 1975; Hallbauer and van Warmelo, 1974; Mossman et al., 2008), whereas others have proposed that they represent the residues of hydrocarbon liquids (Drennan et al., 1999; Drennan and Robb, 2006; England et al., 2002; Fuchs et al., 2016; Gray et al., 1998). The association of the gold with hydrocarbon seams in the hydrothermal model and hydrothermal remobilization in the modified paleoplacer model is explained by the need of a reductant to destabilize the bisulfide complexes, which is thought to be responsible for gold transport (Phillips and Law, 2000; Phillips and Powell, 2011). Multiple types of oil inclusions preserved in quartz grains shows the evidence that solid organic matter (pyrobitumen) is derived from formerly liquid basin-wide circulating oils.

In the current study, the researchers utilized an analytical workflow of ZEISS Atlas 5 large-area SEM imaging, followed by FIB-SEM nanotomography and (S)TEM, to study the nature of gold, uranium, and hydrocarbon mineralizations from micrometer to nanometer scale. The Atlas 5 SEM imaging (including EDS spot analyses and element distribution mapping) was used to identify hydrocarbons, gold and uranium-bearing minerals in order to investigate their distribution, delicate textures, and growth features (Figure 1). Based on the Atlas 5 dataset, the authors selected gold-bearing uraninite aggregates as targets for 3D nanotomography and FIB extraction for (S)TEM analyses (Figure 2A).

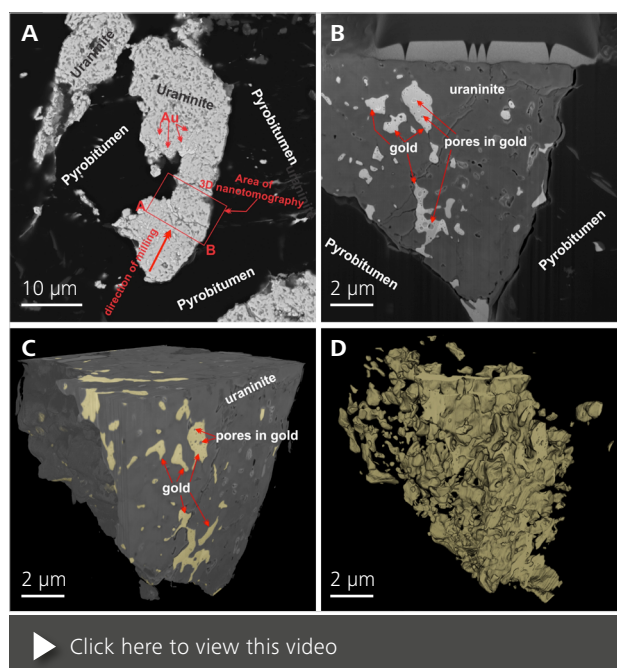


Figure 2 (A) Backscattered electron SEM image of the uraninite aggregate that was selected for FIB-SEM nanotomography and from which the 3D model was produced. The red box indicates the area that was milled to create the 3D model. (B) InLens image from the 3D data set. (C) A reconstructed stack image of the Atlas 3D nanotomography data set showing the uraninite grain with gold in its pore spaces. (D) A reconstructed stack image of the data set with only the gold shown, demonstrating that the gold fills pore space in the uraninite aggregate. The Atlas 3D image data set was segmented, and the grey levels associated with the uraninite aggregate were removed. For better visualization, uraninite and gold were displayed by grey and yellow false colors, respectively.

The latter revealed that aggregates of uraninite nanocrystals host significant volumes of gold in their micro-pores and fractures. All the observed gold grains, in turn, have spherical to ellipsoidal pores which all include uraninite nanocrystals in a thin seam of pyrobitumen (a fossil remnant of crude oil) that lines the inner walls of the pores. The 3D FIB-SEM nanotomography was conducted to visualize the distribution of the enclosed gold grains in the uraninite aggregates as well as the distribution of uraninite- and pyrobitumen-filled pore holes in the gold grains (Figure 2B, C, D; movie clip).

Through the combined use of the above-mentioned suite of methods, and based on the obtained results, the researchers were able to propose a mineralization model for the gold and uranium ore formation. According to this model, formerly liquid hydrocarbons (oil) dissolved uranium and transported it to the site of deposit. In contact with high-temperature, gold-bearing hydrothermal fluids, the two immiscible phases formed oil-in-water micro-emulsions, which triggered the flocculation of uraninite nanocrystals.

The oil droplets in the hydrothermal fluids forced the precipitation of native gold in the pores within large uraninite aggregates due to the chemical reduction of dissolved gold species to native gold. The rapid release and growth of gold crystals entrapped masses of oil droplets that were thermally converted into a pyrobitumen residue.

Materials and Methods

Gold-uraninite, and hydrocarbon-bearing samples from the Carbon Leader Reef in the Witwatersrand basin were imaged with a ZEISS Sigma HD VP field-emission scanning-electron microscope (FE-SEM) at Fibics Incorporated (Ottawa, Canada) using the large-area imaging software ZEISS Atlas 5. The samples were imaged with an accelerating voltage of 14 kV using the backscattered electron (BSE) detector, with a working distance of 11.8 mm, a 7 nA beam current (120 mm aperture), a 1.0 μ s dwell time, and a resolution of 45 nm/pixel. The image mosaic of the sample comprises 2893 images, with each image tile containing 6148 x 6148 pixels (field of view per image approximately 277 x 277 μ m). Several regions of interest were also imaged at a resolution of 5 nm/pixel. Once the large-area image mosaics acquired by the ZEISS Atlas 5 software had been stitched and corrected, the entire datasets were exported to an autonomous series of files called the Browser-Based Viewer (BBV) which allows the user to view the complete dataset at full resolution using a web browser, similar to that of the well-known

Google Earth™ application. The link to the ZEISS Atlas 5 BBV data set of the sample from the Carbon Leader Reef is provided at the end of this manuscript.

High-resolution FIB-SEM nanotomography and energy-dispersive spectroscopic (EDS) analyses were carried out at Fibics Incorporated (Ottawa, Canada) on a Carl Zeiss Crossbeam 540 SEM equipped with a Gemini 2 electron column, a Capella Gallium ion FIB column, and an Oxford Instruments X-MaxN 80 mm² energy-dispersive X-ray spectroscopy (EDS) detector, which was controlled using the Aztec 3.0 software. All nanotomography runs used the Atlas 3D module of the Atlas 5™ software, which allows interlaced milling and imaging. A total of 1212 successive images were captured with an average mill progression of 5 nm per image. The acquired image stacks were loaded into the 3D visualization software “Dragonfly,” rendered into 3D models with 5 nm voxels, and exported into several video files. The video files were loaded into the movie software “Camtasia” and merged into single videos with annotations.

The TEM work was conducted at the Facility for Electron Microscopy Research (FEMR) at McGill University (Montréal, Canada) and the National Research Council (Ottawa, Canada).

Data resources:

Original work

Fuchs, S.H.J., D. Schumann, A.E. Williams-Jones, A.J. Murray, M. Couillard, K. Lagarec, M.W. Phaneuf, H. Vali, 2017: Gold and uranium concentration by interaction of immiscible fluids (hydrothermal and hydrocarbon) in the Carbon Leader Reef, Witwatersrand Supergroup, South Africa. *Precambrian Research*, 293, 39–55, dx.doi.org/10.1016/j.precamres.2017.03.007

The full articles can be downloaded under:

<http://www.sciencedirect.com/science/article/pii/S0301926816304727>

The ZEISS Atlas 5 large area image mosaic can be downloaded under:

<http://www.petapixelproject.com/mosaics/Witwatersrand/CL-N6-exported-BBV/CL-N6-overview/index.html>

The animated movie clip of the 3D nanotomography of the Witwatersrand uraninite grain can be downloaded under:

<http://bit.ly/2ISgmdk>

References:

- Drennan, G.R., Boiron, M.C., Cathelineau, M., Robb, L.J., 1999. Characteristics of post-depositional fluids in the Witwatersrand Basin. *Mineralogy and Petrology*, 66(1-3): 83-109.
- Drennan, G.R., Robb, L.J., 2006. The nature of hydrocarbons and related fluids in the Witwatersrand Basin, South Africa: Their role in metal redistribution. *Geological Society of America Special Papers*, 405: 353-385.
- England, G.L., Rasmussen, B., Krapež, B., Groves, D.I., 2002. Archaean oil migration in the Witwatersrand Basin of South Africa. *Journal of the Geological Society*, 159: 189-201.
- Fuchs, S., Williams-Jones, A.E., Jackson, S.E., Przyblowicz, W., 2016. Metal distribution in pyrobitumen of the Carbon Leader Reef, Witwatersrand Supergroup, South Africa: Evidence for liquid hydrocarbon ore fluids. *Chemical Geology*, 426: 45-59.
- Gray, G.J., Lawrence, S.R., Kenyon, K., Cornford, C., 1998. Nature and origin of "carbon" in the Archean Witwatersrand Basin, South Africa. *Journal of the Geological Society*, 155(1): 39-59.
- Hallbauer, D.K., 1975. Plant origin of the Witwatersrand carbon. *Minerals Science and Engineering*, 7(2): 111-131.
- Hallbauer, D.K., van Warmelo, K.T., 1974. Fossilized plants in thucholite from Precambrian rocks of the Witwatersrand, South Africa. *Precambrian Research*, 1(3): 199-212.
- Mossman, D. et al., 2008. The indigenous origin of Witwatersrand "carbon". *Precambrian Research*, 164(3-4): 173-186.
- Phillips, G.N., Law, J.D.M., 2000. Witwatersrand gold fields: geology, genesis, and exploration. *Reviews in Economic Geology*, 13(13): 439-500.
- Phillips, G.N., Powell, R., 2011. Origin of Witwatersrand gold: a metamorphic devolatilisation–hydrothermal replacement model. *Applied Earth Science*, 120(3): 112-129.



Carl Zeiss Microscopy GmbH
07745 Jena, Germany
microscopy@zeiss.com
www.zeiss.com/microscopy



Not for therapeutic, treatment or medical diagnostic evidence. Not all products are available in every country. Contact your local ZEISS representative for more information.
EN_42_013_263 | CZ 07-2018 | Design, scope of delivery and technical progress subject to change without notice. | © Carl Zeiss Microscopy GmbH